www.cad-journal.net
Computer-Aided Design AND APPLICATIONS™

Application Perspectives of Induction Surfaces in CAD, Smooth Connection of Concentric Spherical Surfaces

Levente Lócsi[1]

[1]ELTE Eötvös Loránd University, Budapest, Hungary, locsi@inf.elte.hu

Corresponding author: Levente Lócsi, locsi@inf.elte.hu

Abstract. Induction sets were recently introduced to observe the effect of linear transformations (multiplication by matrices) on the norm of vectors in more detail. The aesthetics and peculiar properties of induction curves and surfaces provide them with good potential for future application in Computer-Aided Geometric Design. In the present work, we explore the topic of connecting segments of concentric spherical surfaces in a smooth manner. We show that by using the maximum norm and applying diagonal matrices we immediately arrive at concentric spherical sections of different radii with continuous connection in between, but by lowering the norm to a finite but considerably large value we get a smooth connection.

Keywords: induction surfaces, concentric spherical surfaces, smooth connection
DOI: https://doi.org/10.14733/cadaps.2025.700-710

1 INTRODUCTION

Induction surfaces were recently introduced to observe the effect of linear transformations (multiplication by matrices) on the norm of vectors in more detail [5]. Specifically, they visualize for each spatial direction the multiplication factor of the result vector's norm compared to the original vector. In a planar setting, one would arrive at induction curves, and in a general n-dimensional setting induction sets, induction manifolds were defined. The aesthetics and peculiar properties of induction curves and surfaces provide them with good potential for future application in Computer-Aided Geometric Design. The presence of so-called p-eigenvectors and p-eigensubspaces further enrich their interesting properties [7, 6].

In the present work, after giving the definition and some examples of such geometric objects, we explore the topic of connecting segments of concentric spherical surfaces in a smooth manner. We show that by using the maximum norm (as the p-norm in the definition of induction surfaces) and applying diagonal matrices we immediately arrive at concentric spherical sections of different radii with continuous connection in-between. Lowering the norm to a finite but considerably large value we get a differentiable connection, sacrificing however the exactness of the spherical subsurfaces. This smoothing effect is similar to that of Catmull–Clark and Doo–Sabin subdivision surfaces [1, 2], but here we have explicit surfaces (in spherical coordinates), not meshes, nor splines.

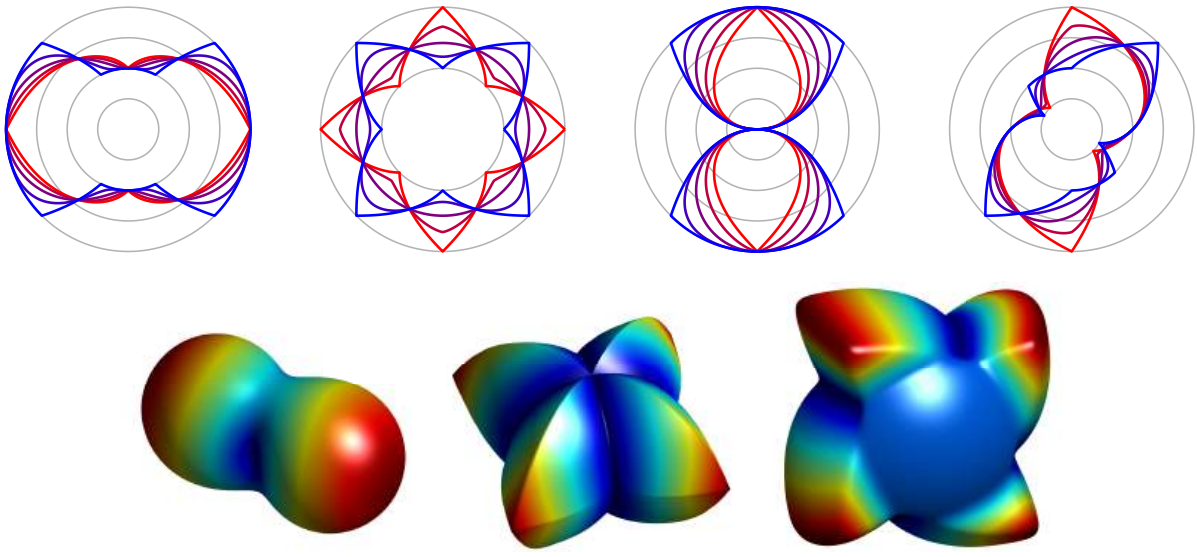

Figure 1: Top row. Some examples of induction curves, from left to right: diagonal matrix, rotation matrix, singular diagonal matrix, and skew matrix. Gray circles denote the radial units, red to blue colors correspond to varying p values with 1, $4/3$, 2, 4, $+\infty$. Bottom row. Some induction surfaces for various matrices and p values with code names "peanut", "compass" and "propeller".

The artistic possibilities are also to be explored further, similarly as seen in the planar case for Pythagorean hodograph curves in Klár–Valasek's [3]. Application possibilities of the current exploration include visualizing solid spherical objects with emphasis on a peculiar set of layers, such as in geology (structure of the Earth) or physics. Witnessed solutions so far used only planar sections between spherical parts lacking any degree of smoothness.

2 THE DEFINITION OF INDUCTION CURVES AND SURFACES

The p-norms or power norms for vectors are used as in general with $2 \leq n \in \mathbb{N}$ as follows:

$$\|.\|_p : \mathbb{R}^n \to \mathbb{R}, \qquad \|x\|_p = \left(\sum_{k=1}^{n} |x_k|^p \right)^{1/p} \qquad (p \in [1, \infty)) \,,$$

and

$$\|x\|_\infty = \max_{k=1}^{n} |x_k| \,.$$

It is well known that $\lim_{p \to +\infty} \|x\|_p = \|x\|_\infty$ $(x \in \mathbb{R}^n)$. Let us now consider a matrix $A \in \mathbb{R}^{n \times n}$. The p-norm of A is defined as follows ("induced" by the vector p-norm):

$$\|.\|_p : \mathbb{R}^{n \times n} \to \mathbb{R}, \qquad \|A\|_p = \sup_{x \neq 0} \frac{\|Ax\|_p}{\|x\|_p} \qquad (p \in [1, \infty]) \,.$$

As an equivalent description one may consider the supremum only for the elements of the unit sphere, i.e. $\|x\|_p = 1$, thus the fraction becomes unnecessary. In this work, we restrict ourselves for $n = 2$ and 3.

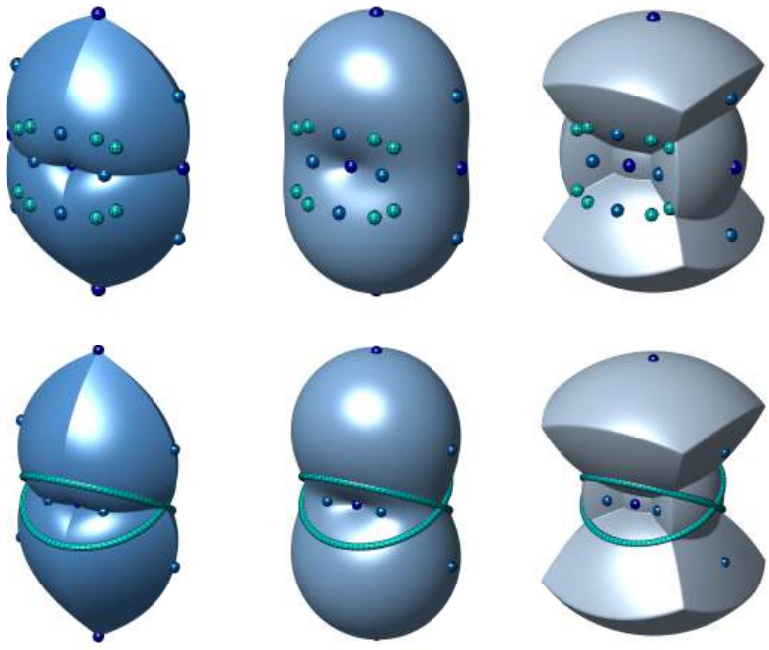

Figure 2: Induction surfaces for two diagonal matrices (rows) with three different p-norms (columns). The common intersection points and curves of the surfaces row-wise are marked.

Let us now define *induction sets* in general, with $n = 2$ resulting in *induction curves* and $n = 3$ in *induction surfaces*. Given a matrix $A \in \mathbb{R}^{n\times n}$ with $2 \leq n \in \mathbb{N}$ and $p \in [1, +\infty]$, the set of points

$$\mathcal{I}_p(A) := \left\{ \frac{\|Ax\|_p}{\|x\|_p} \cdot \frac{x}{\|x\|_2} \in \mathbb{R}^n \ : \ 0 \neq x \in \mathbb{R}^n \right\} \subset \mathbb{R}^n$$

is called the *induction set* of A with parameter p. Instead of all (but the zero) vectors we may consider only one vector for each direction (e.g. the one with norm 1) since the expression $x/\|x\|_2$ is present in the definition. And thus the formula tells us to examine for each direction the fraction $\|Ax\|_p / \|x\|_p$, i.e. what is the multiplication factor for the change in the norm after multiplying our vector with the matrix.

Finally, for each direction we will have one point on a continuous curve or surface around the origin (for regular matrices). It is easy to see that we get a symmetric object with respect to the origin. For a more detailed description and properties we refer to [5].

Fig. 1 presents some (sets of) examples of induction curves and induction surfaces. Matlab programs were used to generate these images, available under https://locsi.web.elte.hu/indsets/.

3 INDUCTION SURFACES OF DIAGONAL MATRICES, WITH P-EIGENVECTORS

We highlight here two more sets of images of induction surfaces with our purpose being twofold. On one hand, this showcases an interesting property of the given surfaces, related to p-eigenvectors, on the other hand, some of these images serve as the primary motivation for our current exploration.

Fig. 2 shows 3+3 induction surfaces for the diagonal matrices $\mathrm{diag}(1, 2, 3)$ and $\mathrm{diag}(1, 2, 4)$ with norms $p = 1,\ 2,\ +\infty$. Although only the surfaces with these three norms are presented, any p value in the interval

$[1, +\infty]$ could have been used. (Actually also between 0 and 1.) It is encouraged to imagine now the smooth transition between these surfaces as p visits $[1, +\infty]$ with the "key frames" as depicted. A similar transition for the induction curves on Fig. 1 (red to blue, for all four sets of curves) may be considered.

Varying the parameter p as described above for fixed matrices led to the discovery of p-eigenvectors. Visually these are points that are common intersections of all the infinitely many curves/surfaces depending on $p \in [1, +\infty]$. These common intersection points corresponding to p-eigendirections can be observed in case of the induction curves of Fig. 1, and are marked with small spheres on Fig. 2. In the case of some special matrices the constellation of these directions blends to form a p-eigensubspace, visually one (or rather two) common intersection curve(s) of all infinitely many surfaces. For a more detailed treatment of this topic see [5, 7].

Now we are motivated by the surfaces (and curves) for diagonal matrices with $p = +\infty$. As it can be seen—and was also confirmed mathematically—these include spherical partial surfaces (circular partial curves). These are concentric, and the radii are exactly the diagonal elements of the matrix. The segments are situated symmetrically around the axes. Furthermore, these segments are connected continuously.

4 SMOOTH CONNECTION OF CONCENTRIC SPHERICAL SURFACES

As seen in the previous section, induction surfaces of diagonal matrices with $p = +\infty$ norm give us spherical surface segments with a continuous connection in between. Applying norms with high p values will smooth our surface at hand, providing a differentiable transition between the spherical segments, sacrificing however the exactness of the original spherical parts. In the following sections we show many examples of induction surfaces highlighting their visual potential and providing informal descriptions, then in Section 4.4 we elaborate on the error introduced in the spherical parts by the smoothing process.

4.1 Three Different Radii

Fig. 3 illustrates this smoothing process in case of the diagonal matrix $\mathrm{diag}(4, 5, 6)$. We start off with the "original" surface with $p = +\infty$ having exact spherical segments (with radii 4, 5 and 6) and their continuous connection, then the subsequent images reduce the value of p to the power-of-two values 64, 32, 16, 8 and 4. The distance of the points from the origin is indicated by colors. Now the colors of the national flag of Hungary (red, white, green) were chosen to honor the location of the CAD'24 conference.

One may observe the gradually more smooth surfaces, but also the decay of the accuracy of the exact spherical sections. Although the colors suggest that the original radii are mostly kept inside the regions of interest. Note that the exact radii are only preserved along the axes, as shown by the theory behind. The appropriate parameter value (for smoothness) may be chosen depending on the application's purpose.

A similar example is given in Fig. 4 with some shades of blue using again 3 different radii, namely 10, 11 and 12, now in a different constellation. The values for p are the same. Since the radii are now relatively close to one another, we may now see that the overall figure is more spherical. Nevertheless, the smoothing process is essentially the same: with the maximum norm we see sharp edges, with lower norm parameters we experience increased smoothness. The final figures in the sets even tend to lose the defined shape of being composed of different spheres. Therefore parameter values below 10 are not recommended, however, they may also have their area of application.

4.2 Two Different Radii: Island, Variations, Stamps

Naturally, if two elements of the diagonal matrix are the same, then we will have an induction surface composed basically of two concentric spheres with two different radii. If all three elements were the same, then we would arrive at a sphere—independent of the norm—which is now of negligible interest.

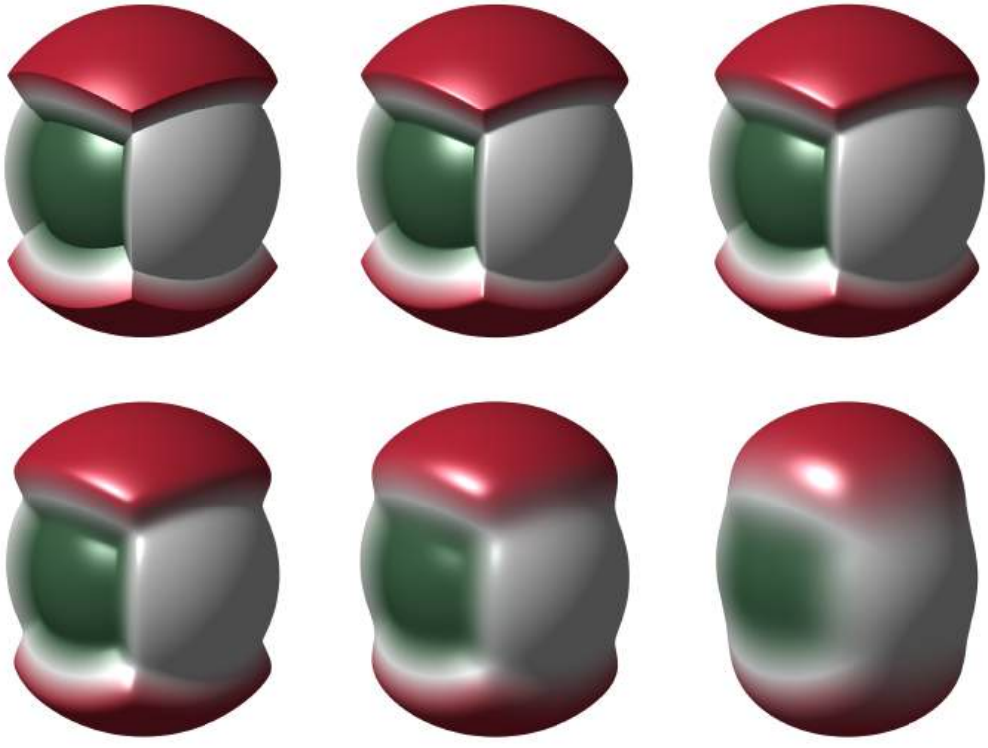

Figure 3: Continuous and smooth connection of concentric spherical segments as given by induction surfaces of diagonal matrices with decreasing p values. Colors indicate the distances from the origin.

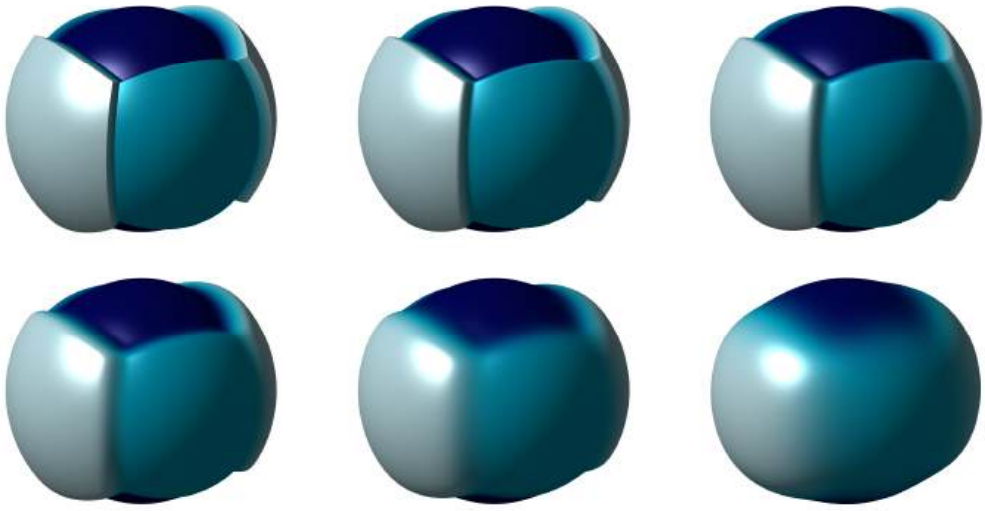

Figure 4: Another example of continuous and smooth connection of concentric spherical segments, now in a different setting, with shades of blue. The parameter values are the same as above.

In this section we discuss the case when two matrix elements are the same, and the third one is bigger. We have chosen the upward direction for the bigger value, thus the result slightly resembles an island surrounded by the sea. The colors will enhance this resemblance. We only plot the upper hemisphere to save space and to give further points of view on application perspectives. On Fig. 5 we see three images based on the matrix $\mathrm{diag}(1,1,2)$ and $p=16$, so already smoothed.

- The first image shows the plain induction surface by the definition. One may observe the square-like border of the upper region similar to the borders on the previous figures.
- The second image is a variation when the radial distances are independent of the azimuthal angle: only the value at the zero angle is considered and used for all angles. With this approach, we get a surface that has rotational symmetry along the vertical axis. As if an induction curve was revolved around its longer axis.
- On the third image we started with the settings of the second image but applied also an argument transformation to see less of the top area and more of the smaller sphere. Basically, the elevation angles where the induction fraction is calculated are moved farther from the upward direction. More formally $\|Av\|_p \,/\, \|v\|_p$ is calculated not simply for $v=(\cos\varphi,\sin\varphi),\ \varphi\in[0,\pi/2]$ on a vertical plane but for

$$v=\begin{pmatrix}\cos\,t_\gamma(\varphi)\\ \sin\,t_\gamma(\varphi)\end{pmatrix}\quad\text{with}\quad t_\gamma\colon[0,\pi/2]\to[0,\pi/2],\quad t_\gamma(\varphi)=\mathrm{sgn}(\varphi)\cdot\frac{\pi}{2}\cdot\left(\frac{|\varphi|}{\pi/2}\right)^{\gamma}.$$

  This time $\gamma=2$ was used. In general $\gamma\in(0,+\infty)$.

Figure 5: Variations on induction surfaces with code name "island". Two elements of the inducing diagonal matrix are the same and the third one (corresponding to the upward direction) is bigger. From left to right: basic induction surface, a variation with rotational symmetry, a transformed version with a smaller top region.

Fig. 6 showcases a number of examples of the transformed induction surfaces with similar settings. Now we assign the name "stamp". From left to right, we see increasing smoothness of the surfaces using parameters $p=32,16,8$. In the rows we have the below matrices and γ parameters for the argument transform:

- $A_1=\mathrm{diag}(2,2,3),\ \gamma=1$;
- $A_2=\mathrm{diag}(1,1,2),\ \gamma=2$;
- $A_3=\mathrm{diag}(1,1,3),\ \gamma=3$;
- $A_4=\mathrm{diag}(1,1,4),\ \gamma=4$.

So compared to a base level, the elevation has respectively 1.5, 2, 3 and 4 times the radius. The small (approximately) spherical segments with rounded edges at the top start to get hard to distinguish from a flat surface.

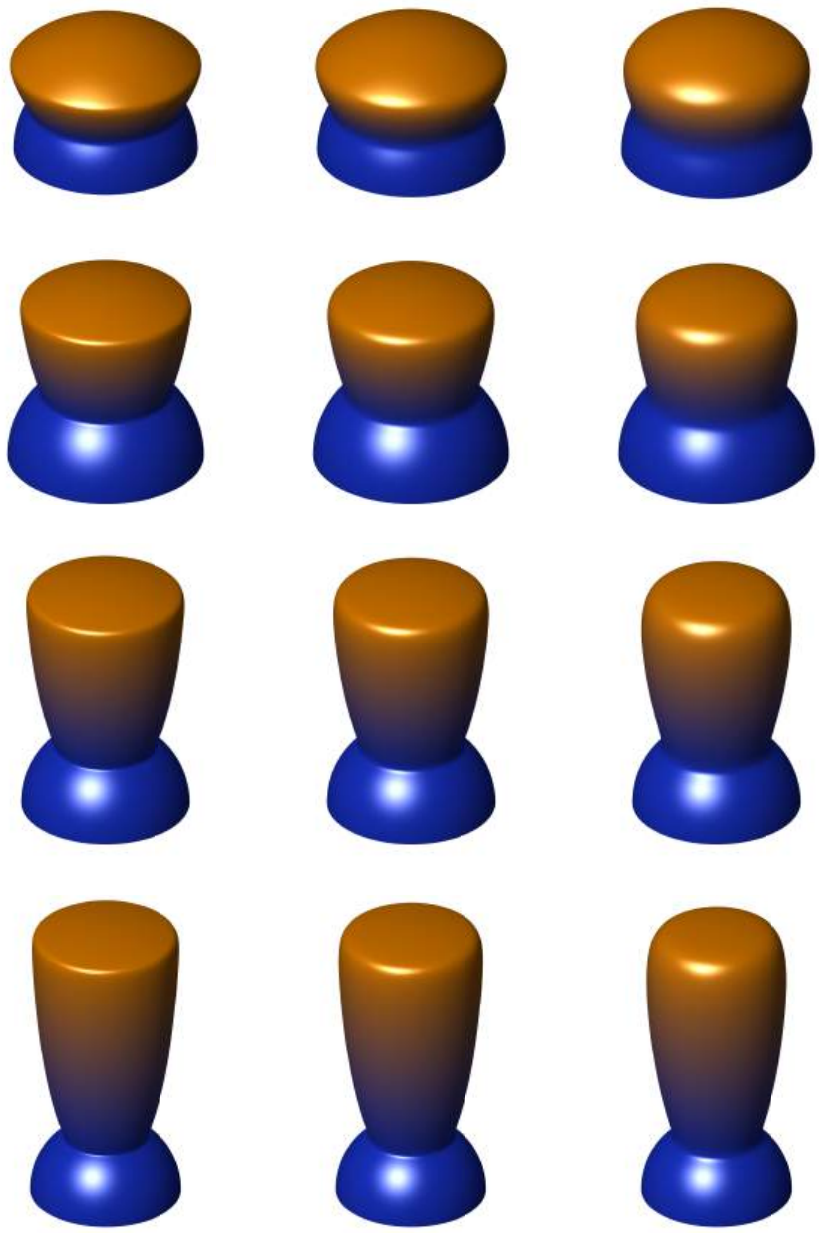

Figure 6: Variations on induction surfaces similar to stamps. Two elements of the inducing diagonal matrix are the same and the third one is bigger. From left to right: the smoothness increases. From top to bottom: the ratio of the radii (and the transform's parameter) gets larger.

4.3 Two Different Radii: Eggs

Let us now examine the case when two elements of the diagonal matrix are the same, and the third one is smaller, specifically $\mathrm{diag}(3, 3, 2)$. Again we have chosen the upward direction for the smaller value, thus the result looks like a hole in the ground. We have chosen the variation with rotational symmetry for demonstration, transformed as above with parameter $\gamma = 0.75$ to make the smaller sphere more visible. This time we used yellow and white colors, and top and side views for the examples seen in Fig. 7 resembling a "fried egg". In case of these simple views from coordinate directions, we let the shading tell most of the story of increasing smoothness while the parameter p takes the values $+\infty$, 40, 20 and finally 10.

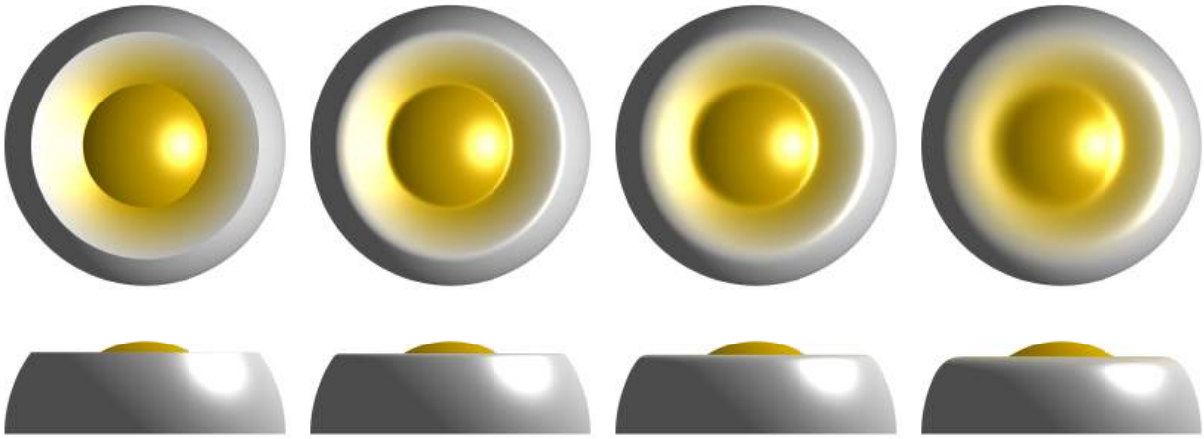

Figure 7: Variations on induction surfaces: eggs. Two elements of the inducing diagonal matrix are the same and the third one is smaller. From left to right: the smoothness increases. Top and side views are presented.

4.4 The Error in the Spherical Segments

The maximum norm will give us exact spherical segments connected continuously but not in a differentiable manner. Reducing the value of the parameter p we experience a smooth connection, but the exactness of the spherical subsurfaces is degraded. The exact radius is only kept in the coordinate directions (6 points), although if p is still considerably large, then the error is hardly observable. Naturally, questions arise about the amount of the error of the (almost) spherical segments. In this section, we give a qualitative description of the error using some of the examples in Fig. 3 by modifying the coloring.

In Fig. 8 we show the induction surfaces (now only on one octant) of the matrix $\mathrm{diag}(4, 5, 6)$ again with parameter $p = 32$, 16, 8 respectively, but now the coloring has some steps introduced, which results in some darker stripes on the surfaces. The steps were introduced as follows. We created a 201 step colormap with red and green at the ends of the scale, white in the middle, and linearly interpolated colors in between. Then the 2nd, 4th, and 6th elements were darkened, and similar was done at the end, and near the middle. So the first stripes will appear when the radius is closer to 4.01 instead of 4, or to 5.99 instead of 6.

We may observe that in the case of these parameters, the radii at the spherical subsurfaces are mostly kept within 0.01 error. In case of $p = 32$, almost the complete spherical part stays within this threshold. But in case $p = 8$ the area with this small amount of error is considerably shrunken. The setting $p = 16$ results in a middle ground: the smoothness is already quite visible, but a lot of the spherical parts are within a 0.01 error bound.

Figure 8: Visualizing the error of the spherical subsurfaces for varying smoothness. A stripe corresponds to about 0.01 difference in radial distance. (The red radius is 6, white is 5 and green is 4.) $p = 32, 16, 8$.

To have a more clear view of the error we present Fig. 9. Induction curves of the matrix $\mathrm{diag}(2, 1)$ are shown on the first quadrant with parameter values $p = +\infty, 32, 16, 8$. These curves may be also considered as cross-sections of the induction surfaces as above (mind the different ratios of radii). Exact circular arcs can be seen for $p = +\infty$ with a curve connecting them continuously. The next images don't show exact circular arcs anymore (except for the polar grid lines) but are very close, and the smooth connection may now be observed.

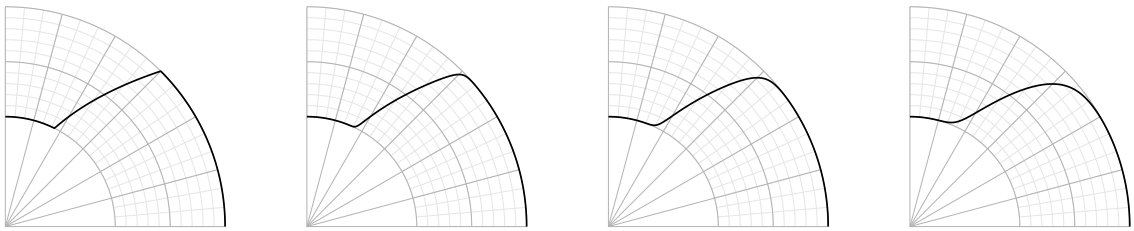

Figure 9: A planar visualization of the error. Induction curves with increasing smoothness. $p = +\infty, 32, 16, 8$.

5 DISCUSSION AND FURTHER WORK

We argue that the recently introduced induction surfaces may have potential application perspectives in Computer-Aided Geometric Design. Specifically, the induction surfaces of diagonal matrices with the maximum norm have concentric spherical surfaces connected continuously. Furthermore reducing the parameter p of the norm to a finite but considerably large value (mostly between 16 and 64) results in a smooth connection of the spherical subregions, which are only slightly altered. Considering spherical coordinates these surfaces are defined explicitly, not via meshes or splines. However for the illustration here, we created meshes based on elevation and azimuthal angles, the parametric description of the sphere.

Although induction surfaces provide an elegant way to connect concentric spherical surfaces, the locations of these spherical parts were also provided by the induction sets at hand, depending on the initial diagonal matrix. One may observe that a bigger radius gives rise to a bigger surface with this radius, and vice-versa, smaller segments are present with a smaller radius. And these segments were always situated around the axes. From an application perspective, it would be desired that the location and size of the spherical surfaces

could be also prescribed by the user and then connect the given parts. Now we have applied an argument transform in the special case when two elements of the initial diagonal matrix were the same. However, after this transformation, the surface loses its explicit nature and is rather described in a parametric form.

A direction of further research is to describe a way to solve the problem of applying induction surfaces to connect concentric spherical surfaces as prescribed by a user. One approach would be to use argument transformations not just for one but two variables, some suitable bijection of the unit sphere onto itself (or a group of these with respect to composition) [4, 8]. Another approach is to transform the radii for each direction after we have an induction surface, e.g. squaring the radii would leave the spherical areas the same, but alter the radial distances.

Yet another closely related problem would be to describe a method using induction surfaces to visualize such concentric spherical surfaces smoothly connected which are revealed in larger and larger circular areas (c.f. Fig. 7), or having more than 3 different radii present.

A natural generalization in a rather mathematical direction would be the smooth connection of non-concentric spherical surfaces. One approach could be the utilization of the Poincare sphere model of the Bolyai–Lobachevsky hyperbolic geometry, Blaschke functions, and their generalizations [4, 8]. A different approach could be a Doppler-like transformation.

From a computer graphics point of view one could elaborate faster and more effective methods to visualize induction sets (and apply them as a solution to some problems). Currently, we created meshes based on spherical coordinates for the visualization, and this results in more dense mesh points along the north and south poles. More elaborate meshes (even dynamically created) may be considered. The use of signed distance functions and distance fields is worth examining as well.

Application possibilities of the current exploration include visualizing solid spherical objects with emphasis on a peculiar set of layers, such as in geology (structure of the Earth) or physics. One may also add noise or texture to parts of the surfaces at hand for increased visual impact as in Fig. 10.

The loss of precision in the spherical sections may be also further examined and quantified.

Of course, there are many further questions posed already regarding induction sets and p-eigenvectors not directly related to CAD [5, 7, 6].

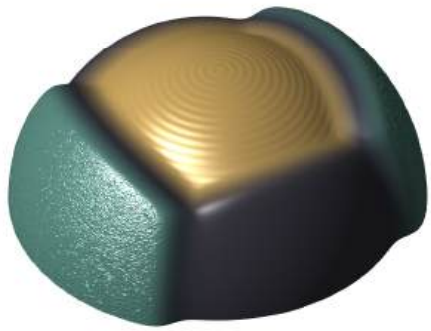

Figure 10: An example with added texture (waves and noise).

6 CONCLUSIONS

The potential application areas of induction curves and induction surfaces in Computer-Aided Design are yet unexplored. However, these explicit surfaces may prove useful for the solution of some specific problems. Also, their aesthetics and special properties make them worth studying for the design of visual elements.

In this work, we have shown that induction surfaces may be used to provide a continuous and even smoothed connection between concentric spherical segments. Several directions for further research were listed. Foremost the problem of connecting user-specified concentric spherical sections (or at least give an appropriate approximation) is yet to be examined.

The Matlab programs that were used to create the images in this article (and for further related research) are available under https://locsi.web.elte.hu/indsets/.

Levente Lócsi, https://orcid.org/0000-0002-6786-8467

REFERENCES

[1] Catmull, E.; Clark, J.: Recursively generated b-spline surfaces on arbitrary topological meshes. Computer Aided Design, 10(6), 350–355, 1978. http://doi.org/10.1016/0010-4485(78)90110-0.

[2] Doo, D.; Sabin, M.: Behaviour of recursive division surfaces near extraordinary points. Computer Aided Design, 10(6), 356–360, 1978. http://doi.org/10.1016/0010-4485(78)90111-2.

[3] Klár, G., G.; Valasek: Employing Pythagorean hodograph curves for artistic patterns. Acta Cybernetica, 20, 101–110, 2011. http://doi.org/10.14232/actacyb.20.1.2011.8.

[4] Lócsi, L.: A hyperbolic variant of the Nelder–Mead simplex method in low dimensions. Acta Universitatis Sapientiae, Mathematica, 5(2), 169–183, 2013. http://doi.org/10.2478/ausm-2014-0012.

[5] Lócsi, L.: Introducing p-eigenvectors, exact solutions for some simple matrices. Ann. Univ. Sci. Budapest. Sect. Comput., 49, 325–345, 2019.

[6] Lócsi, L.: Identification of induction curves. Stud. Univ. Babeş–Bolyai Math., 68(3), 467–480, 2023. http://doi.org/10.24193/subbmath.2023.3.01.

[7] Lócsi, L.; Németh, Z.: On the construction of p-eigenvectors. Ann. Univ. Sci. Budapest. Sect. Comput., 50, 231–247, 2020.

[8] Pap, M.; Schipp, F.: Quaternionic Blaschke group. Mathematics, 7(1), 33, 2019. http://doi.org/10.3390/math7010033.